Crystal Structures of Complexes of a Peptidic Inhibitor with Wild-Type and Two Mutant HIV-1 Proteases[†,‡]

Lin Hong,[§] Annemarie Treharne,[§] Jean Ann Hartsuck,[§,||] Steve Foundling,[§] and Jordan Tang*[,§,||]

Protein Studies Program, Oklahoma Medical Research Foundation, and Department of Biochemistry and Molecular Biology, University of Oklahoma Health Sciences Center, Oklahoma City, Oklahoma 73104

Received February 27, 1996[⊗]

ABSTRACT: Crystal structures of the protease of human immunodeficiency virus type 1 (HIV-1) and two mutant proteases, V82D and V82N, have been determined. In all three cases the enzyme forms a complex with the peptidic inhibitor U-89360E. All structures have been determined to 2.3 Å resolution and have satisfactory agreement factors: 0.173 for wild type, 0.175 for V82D, and 0.182 for V82N. Comparison of the three crystal structures provides explanations which are consistent with the known kinetic properties of these mutant enzymes with the U-89360E inhibitor [Lin, Y., Lin, X., Hong, L., Foundling, S., Heinrikson, R. L., Thaisrivongs, S., Leelamanit, W., Raterman, D., Shah, M., Dunn, B. M., & Tang, J. (1995) *Biochemistry 34*, 1143−1152]. Unfavorable van der Waals interactions between the inhibitor and the mutated side chains at position 82 are consistent with diminished affinity for the inhibitor by the mutant enzymes. If a mutation is potentially resistant to an inhibitor, the mutant enzyme should not only have an increased K_i for the inhibitor but should also preserve considerable catalytic capability. The V82D mutant possesses these qualities. In the V82D crystal structure, a water molecule, which connects the protease flap to the inhibitor, is missing or of low occupancy. Absence of this bridge may be important in determining catalytic capability. Moreover, mutation at position 82 induces change in two polypeptide backbone regions, 35−41 and 67−68, which may be related to protease flap mobility.

The activity of the protease of human immunodeficiency virus type 1 (HIV-1)[1] is essential for the maturation of new virions and infectivity of the virus (Kohl *et al.*, 1988; Peng *et al.*, 1989). For this reason, the enzyme is regarded as a primary target for AIDS therapy. Many potent and specific inhibitors for this enzyme have now been designed, synthesized, and tested (Debouck & Metcalf, 1990; Petteway *et al.*, 1991; Tomasselli *et al.*, 1991; Huff, 1991; Wlodawer & Erickson, 1993). *In vitro*, *in vivo*, and clinical experiments confirm that some of these inhibitors have anti-HIV properties (Ashorn *et al.*, 1990; Roberts *et al.*, 1990; Kempf *et al.*, 1990; Vacca *et al.*, 1991) and are potential drugs for treating AIDS.

A serious impediment for the drug therapy against HIV-1 is the ability of the virus to develop drug resistance [for reviews, see Mellors *et al.* (1995) and Ridky and Leis (1995). This was first observed for the reverse transcriptase inhibitors in which the resistance was attributable to mutations in the substrate binding site of this enzyme. In the case of HIV-1 protease inhibitors, resistant strains with mutations of the protease have been observed from HIV-1 grown in cell culture in the presence of inhibitors [for review, see Erickson (1995)]. Moreover, clinical studies have shown that resistant strains emerge after a few weeks of administration of protease inhibitor drugs (Wei *et al.*, 1995; Ho *et al.*, 1995). As a consequence of the high replication rate of the virus, the strains containing mutated protease resistant to the inhibitors are rapidly selected (Condra *et al.*, 1995).

Mutant HIV-1 proteases confer resistance to an inhibitor by retaining sufficient catalytic activity while reducing sensitivity to inhibition. Since this differential modulation of enzymic properties is a manifestation of structure−function relationships among the mutant enzymes, a number of laboratories have undertaken the study of mutant enzyme kinetics (Lin *et al.*, 1995; Gulnik *et al.*, 1995) and crystal structures (Baldwin *et al.*, 1995; Chen *et al.*, 1995). To analyze the catalysis and inhibition of the wild-type and mutant HIV-1 proteases, we previously developed a kinetic model for quantitative comparison of mutation−resistance relationships (Tang & Hartsuck, 1995). Using this model as a guide, we have chosen to determine X-ray crystal structures of wild-type protease and mutant enzymes V82N and V82D; each is in complex with the HIV-1 protease inhibitor U-89360E. The aim is to understand the structural basis of mutational resistance in HIV-1 protease. For complexes with U-89360E, the kinetic data are k_{cat}/K_M = 0.275, 0.098, and 0.011 μM^{-1} s^{-1} and K_i = 20, 560, and 2100 nM for wild-type, V82D, and V82N proteases, respectively (Lin *et al.*, 1995). The model suggests that wild-type and V82N proteases are adequately inhibited by U-89360E whereas V82D is a putative resistant mutation.

EXPERIMENTAL PROCEDURES

Wild-Type and Mutant Enzyme Preparation and Purification. The recombinant wild-type, V82D, and V82N HIV-1 proteases were expressed in *Escherichia coli* as previously described (Ido *et al.*, 1991; Lin *et al.*, 1995) with minor modifications. Briefly, *E. coli* strain BL21(DE3)pLysS

[†] This work was supported by NIH Grant AI-38189.

[‡] The atomic coordinates for these structures have been submitted to the Protein Data Bank. The PDB File Names are 1GNO for the wild-type, 1GNM for the V82D mutant, and 1GNN for the V82N mutant HIV-1 proteases.

* Address correspondence to this author at the Oklahoma Medical Research Foundation, 825 NE 13th St., Oklahoma City, OK 73104. E-mail: Jordan-Tang@omrf.uokhsc.edu. FAX: (405) 271-7249.

[§] Oklahoma Medical Research Foundation.

[||] University of Oklahoma Health Sciences Center.

[⊗] Abstract published in *Advance ACS Abstracts,* July 15, 1996.

[1] Abbreviations: HIV-1, human immunodeficiency virus type 1; AIDS, acquired immunodeficiency syndrome; DTT, dithiothreitol; rms, root mean square.

S0006-2960(96)00481-3 CCC: $12.00

harboring either plasmid pET-3b-HIV-1P (for the wild-type enzyme) or the same plasmid with appropriate base changes (for V82D and V82N) was cultured, and inclusion bodies were prepared. The inclusion bodies were dissolved at a concentration of 10 mg/mL in a solution containing 20 mM Tris, pH 7.5, 8 M urea, and 3 mM DTT and centrifuged at 30000*g* for 15 min. The clear supernatant was passed through a Pharmacia DEAE-Sephacel column previously equilibrated with the same buffer. The fractions of the breakthrough peak, which contained the HIV-1 protease, were pooled and dialyzed against a buffer containing 20 mM chloroacetic acid/sodium acetate, pH 3.0, 8 M urea, and 3 mM DTT. The dialyzed sample was then loaded onto a SynChropak S 300 cation-exchange HPLC column which was preequilibrated with the same buffer and eluted with a linear gradient of 0−500 mM NaCl in the same buffer. The HIV-1 protease peak, which emerged at 250 mM NaCl, was pooled and dialyzed overnight at 4 °C against a refolding buffer (for the wild-type and V82N enzymes, 10 mM sodium phosphate, pH 6.8, with 1 mM DTT; for V82D, 10 mM sodium acetate, pH 5.0, with 1 mM DTT). This solution, which contained the refolded protease, was centrifuged at 30000*g* for 20 min to remove the small amount of insoluble material. The soluble protease in the supernate was subjected to further chromatography on a Pharmacia SP-Sepharose FPLC column which was eluted with a 0−300 mM NaCl linear gradient in 10 mM sodium phosphate, pH 6.8, with 1 mM DTT and 1% glycerol. The protease was eluted at 200 mM NaCl. Ten percent (v/v) glycerol was added to the protease-containing fractions which were stored at −70 °C. Homogeneity of the final sample was confirmed by SDS−polyacrylamide gel electrophoresis.

Crystal Growth. The inhibitor U-89360E, a gift of the Upjohn Co., was dissolved in dimethyl sulfoxide at 25 mg/mL. The protease solutions were prepared as follows: for wild type, 4.0 mg/mL in 1 mM DTT and 10 mM sodium phosphate, pH 6.5; for V82D, 4.6 mg/mL in 1 mM DTT and 20 mM sodium acetate, pH 4.0; for V82N, 5.0 mg/mL in 1 mM DTT and 20 mM sodium acetate, pH 5.5. The enzyme solutions were mixed with a 10-fold molar excess of inhibitor and incubated for a least 2 h at room temperature. Crystallization experiments employed the hanging drop technique using equal volumes of protein−inhibitor solution and well solution in the drops. For all three enzymes, a grid screen of crystallization conditions, which ranged from 18% to 38% $(NH_4)_2SO_4$ and from pH 5.8 to pH 7.3, was accomplished with 200 mM sodium phosphate/citric acid buffers. Ten percent dimethyl sulfoxide, 30 mM β-mercaptoethanol, and 4% 2-propanol (2% for the wild type) had been added to the well solutions. Crystals grew after a few weeks. The most favorable crystallization conditions were as follows: for wild type, 34% $(NH_4)_2SO_4$, pH 7.3; for V82D, 20% $(NH_4)_2SO_4$, pH 5.8; for V82N, 38% $(NH_4)_2SO_4$, pH 5.8.

Crystal Structure Determinations. For each protease−inhibitor complex, a full set of diffraction data was collected from one single crystal on a Siemens multiwire, position-sensitive area detector mounted on a four-circle goniometer. X-rays were generated by a direct drive rotating anode source operated at 50 kV and 100 mA equipped with a graphite monochromator to produce Cu Kα radiation. Diffraction data were recorded, visualized, and reduced using the Siemens software packages FRAMBO and SAINT. All three crystals had hexagonal diffraction patterns. Previously determined, apparently isomorphous HIV-1 protease−inhibitor crystal structures have been solved in either space group $P6_1$ (Erickson *et al.*, 1990; Abdel-Meguid *et al.*, 1993) or space group $P6_122$ (Murthy *et al.*, 1992). On the basis of the results shown in Table 1, all three structures described herein were reduced and refined in space group $P6_1$. As a consequence of this choice, although the HIV protease monomers are chemically identical, each is treated as an independent unit in the crystal structures. Table 2 contains unit cell parameters and data collection statistics for each of the three crystal structures. Statistical analyses were performed with SAS programs from the SAS Institute, Inc., Cary, NC.

Table 1: Data Reduction Comparison for V82N HIV-1 Protease Diffraction Data[a]

resolution (Å)	R_{sym}[b] for $P6_1$	R_{sym} for $P6_122$
2.13−2.20	0.1145 (386)[c]	0.1276 (494)
2.20−2.29	0.0942 (1895)	0.1020 (1984)
2.29−2.39	0.0893 (2577)	0.0955 (2628)
2.39−2.52	0.0774 (2990)	0.0826 (3058)
2.52−2.68	0.0689 (3403)	0.0734 (3448)
2.68−2.88	0.0509 (3728)	0.0546 (3776)
2.88−3.17	0.0399 (4213)	0.0427 (4246)
3.17−3.63	0.0322 (4751)	0.0342 (4771)
3.63−4.58	0.0353 (13233)	0.0356 (13280)
4.58−33.00	0.0308 (18252)	0.0313 (18200)

[a] Data of this table were subjected to a weighted analysis of variance where the number of nonsinglet observations in the resolution range was used as weights. The R_{sym}'s for space group $P6_1$ are significantly better. For the hypothesis that the space groups fit the data equally well, the probability is 0.029 for all data and 0.0013 for data <2.88 Å. [b] $R_{sym} = \sum\sum|I_{i(h)} - \langle I_{(h)}\rangle|/\sum I_{i(h)}$. [c] Form of the data is R_{sym} (number of nonsinglet observations).

The starting model for the V82N structure refinement consisted of the protein portion of the 2.3 Å structure of HIV-1 protease in complex with the symmetrical inhibitor SB204144 (Abdel-Meguid *et al.*, 1993). The other two structure refinements used the partially refined V82N structure as a starting point. Unless otherwise noted computations were performed in the CCP4 program suite (Bailey, 1994). Crystallographic refinements were carried out using the restrained least-squares program PROLSQ. In each case, several cycles of least-squares refinement using data from 12.0 to 2.8 Å reduced the *R*-factor to about 0.27. Electron density maps with coefficients $2|F_o| - |F_c|$ and $|F_o| - |F_c|$ were calculated and displayed on an Evans and Sutherland PS390 graphics system using FRODO Version 6.6 (Jones, 1978). These maps showed clear inhibitor density. Electron density for inhibitor cyclohexyl rings was readily visualized in both the P_1 and P_1' subsites of the enzyme. Figure 1 shows electron density that clearly establishes the two orientations of the inhibitor for the V82D structure. Consequently, two inhibitor orientations were included in subsequent refinements. The virtually identical occupancies of the two inhibitor orientations were confirmed by the relationship of occupancy and thermal parameters in least-squares refinement (Fitzgerald *et al.*, 1990). Special bond and angle parameters for the inhibitor molecule were incorporated into the PROTIN program of the CCP4 package. Each complex was further refined in steps to a final resolution range of 8.0−2.3 Å. Map inspection and model building were performed after each refinement step. Water molecules were added as identified only if their electron density exceeded 3σ in the $|F_o| - |F_c|$ map and if their contacts with other atoms in the structure did not violate

Table 2: X-ray Crystallographic Statistics

	wild type	V82D	V82N
space group	$P6_1$	$P6_1$	$P6_1$
unit cell (Å)	$a = b = 63.16$, $c = 83.59$	$a = b = 63.17$, $c = 83.80$	$a = b = 63.26$, $c = 83.68$
R_{sym}[a]	0.039	0.044	0.038
data completeness[b] (%) (100−2.3 Å)	90.7	92.5	97
R-factor[c]	0.174	0.175	0.183
rms deviation from ideality (Å)	0.013	0.014	0.014
covalent bond lengths	0.051	0.051	0.053
angle distances			
no. of water molecules	73	100	87
B-factor (Å^2) average for protein atoms	20.2	18.0	20.0

[a] $R_{sym} = \sum\sum|I_{i(h)} - \langle I_{(h)}\rangle|/\sum I_{i(h)}$. [b] Reflections whose intensities were less than 3σ in the data reduction statistics were not included in this analysis or in the subsequent refinements and electron density maps. [c] *R*-factor $= \sum||F_o| - |F_c||/\sum|F_o|$, where F_o and F_c are the observed and calculated structure factors. The *R*-factors are reported for the data range 8.0−2.3 Å.

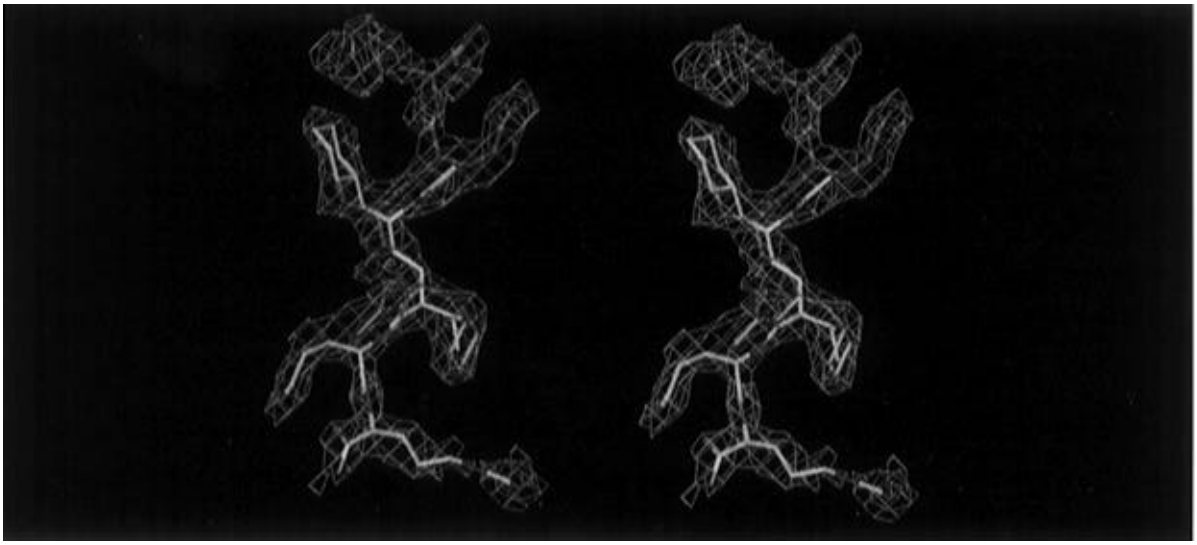

FIGURE 1: Inhibitor structure and electron density. The stereoview shows the two orientations of the U-89360E inhibitor molecule, C in yellow and D in green. Note that the electron density from the two inhibitor molecules overlaps in the central portion of the active site. Contours from the $2|F_o| - |F_c|$ electron density map clearly show two positions for the inhibitor cyclohexyl ring. The dual orientation is substantiated in all three crystal structures, but only the models and density from the V82D complex are shown.

van der Waals radii. Statistical parameters for assessment of the quality of the three enzyme−inhibitor crystal structures are included in Table 2. All three structures were analyzed using the program PROCHECK (Laskowski *et al.*, 1993). In each structure, more than 95% of the residues were in the most favored regions of the Ramachandran plot, and all aggregate main chain and side chain parameters were within 1σ of values expected for this resolution. The refined sets of coordinates have been submitted to the Protein Data Bank (Bernstein *et al.*, 1977). For all comparisons of superposed structures, a significant deviation is defined as greater than 2σ above the mean deviation. Illustrations were prepared with the molecular graphics program O (Jones *et al.*, 1991).

RESULTS AND DISCUSSION

Description of the Protein Structures. The three protein crystal structures described herein are substantially the same. All belong to the same space group and are closely isomorphous (Table 2). In order to evaluate differences in the refined structures, the main chain protein atoms from each of the two mutant crystal structures were aligned with the wild-type structure by means of least-squares, rigid body superposition. No large-scale alteration in main chain folding was observed. After alignment, the rms deviations of the main chain atoms between the wild-type and mutant structures are 0.28 Å for wild type to V82N and 0.29 Å for wild type to V82D. The same measurement is 0.18 Å when the two mutant structures are compared. In subsequent descriptions, the two monomers of the HIV-1 protease molecule are referred to as A and B as previously defined by Wlodawer and Erickson (1993). The two inhibitor molecules in each structure are referred to as C and D.

Compared to the wild-type enzyme structure, each of the mutants displayed significant variance at essentially the same three locations. First, in the wild-type structure, two backbone conformations are observed at the tip of the β-flap which covers the active site. For both mutant structures, there is a hydrogen bond bridging the carbonyl group of residue B50 to the amide of residue A51. For the alternate wild-type conformation, the same carbonyl group points away from the A monomer. These conformational permutations have been observed before in other HIV-1 protease−inhibitor complexes (Wlodawer & Erickson, 1993; Nicholson *et al.*, 1995; Lam *et al.*, 1994). Moreover, ^{15}N NMR relaxation data demonstrate chemical exchange on the millisecond to microsecond time scale at this location in the HIV-1 protease structure in solution. On the basis of these data, Nicholson *et al.* (1995) suggest that the various conformations of the tips of the flaps are in a dynamic equilibrium. Consequently, a disordered crystal structure at this location is not surprising. Second, residues 35−37 and 40 and 41 in both monomers show significant C_α position deviation from the wild-type protease. These residues are in random coil and form a surface loop which connects an

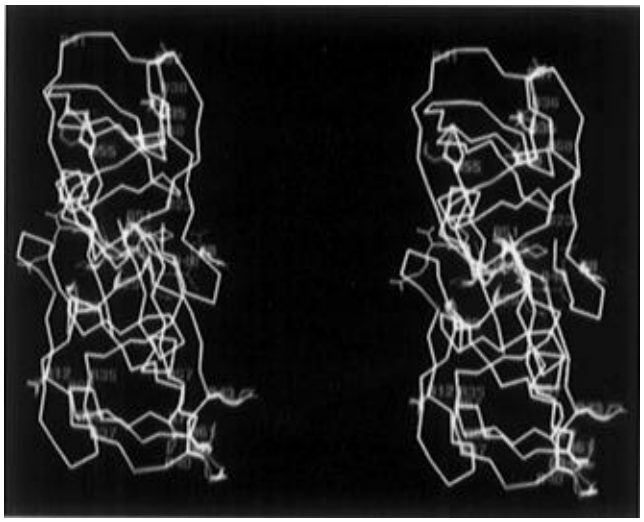

FIGURE 2: C_α superposition for the crystal structures of the wild-type, V82D, and V82N HIV-1 proteases. Where the three structures overlap, the polypeptide backbone appears white. For differences in the structures, individual colors (red for wild type, green for V82D, and blue for V82N) are visible. All regions of significant C_α differences are labeled with green residue labels. Significantly deviant side chains have been added to the figure and labeled in red. For reference, the inhibitor molecules (C in yellow and D in green) and the active site aspartic acid side chains (A25 and B25) from the wild-type structure are included.

interior β-strand to the active-site flap. NMR structural analysis revealed large motions on the nanosecond to picosecond time scale for the amide nitrogen atoms of this loop (Nicholson *et al.*, 1995). This structural lability in solution could well be manifested as conformational variation in the crystal structure. Consistent with structural lability for residues 35−41 of HIV-1 protease, the crystallographic temperature factors for the backbone atoms of these residues average 36, 28, and 33 Å^2 for the wild-type, V82D, and V82N structures, respectively. These backbone temperature factors are the highest in each of the structures and are well above the overall temperature factors (Table 2). Additionally, nonconservative mutagenesis at position 38 diminishes protease activity (Loeb *et al.*, 1989); so there may be a functional relationship between flap interaction with a substrate or inhibitor and conformation of the loop which follows the flap. Finally, in both the A and B monomers, significant deviations in C_α positions are observed for surface residues 67 and 68, located at the end of a β-loop. No particular backbone lability is seen in the NMR structure for these residues. However, internal motion is substantial for the nearby residue 71. Also, molecular dynamics calculations suggest that motion in this β-loop is correlated with flap motion in HIV-1 protease (Harte *et al.*, 1990). The spatial relationships of the residues under discussion are shown in Figure 2.

In contrast to the high degree of similarity described above for main chain conformation among the three structures, there is a greater difference observed when the A and B monomers from one structure are superimposed. Upon alignment of the backbone atoms, the A to B rms deviations are 0.36, 0.34, and 0.32 Å for the wild type, V82N, and V82D, respectively. Careful examination of the electron density maps did not reveal additional orientations for any of the side chains which are deviant. Therefore, even though they are chemically identical, the A and B monomers in these crystals have subtly different conformations and do not arrange themselves randomly in the crystal. The distinction between the A and B monomers of crystallized HIV-1 protease−inhibitor complexes has been documented and discussed previously (Wlodawer & Erickson, 1993). This difference between the two monomers does not confer orientation specificity on the bound inhibitor molecule, as evidenced from our crystals which contain an equal mix of inhibitors with the cyclohexyl ring of the inhibitor molecule situated in binding pockets of both the A and B monomers.

Comparison of the aligned structures demonstrates significant changes in several side chain conformations. Figure 3 identifies those residues whose side chain conformation changes as a result of mutation, and their location in the molecule is shown in Figure 2. Inspection of the graphs in Figure 3 readily substantiates that the V82D and V82N structures are more similar to one another than either is to the wild-type structure. When attention is restricted to deviations greater than 2σ from the mean deviation, virtually the same residues are identified no matter whether V82D or V82N is compared to the wild-type enzyme. A large deviation of the Leu A23 side chain is of particular significance since it is in direct contact with the cyclohexyl ring of the inhibitor. All other residues with significant side chain deviations identified in Figure 3 are on the surface and have little contact with other protein atoms.

Description of the Inhibitor Structures. In each of the three crystal structures, there are two alternate, almost equally occupied, inhibitor orientations. These two orientations are related to one another by the pseudo-2-fold rotation axis which relates the A and B monomers of the enzyme dimer. Consequently, the inhibitor binding modes for two orientations are different. In one inhibitor orientation, the cyclohexyl ring of inhibitor "residue" 2 occupies the P_1 subsite of the enzyme and the valine side chain of inhibitor "residue" 3 occupies the P_1' subsite. In the other inhibitor orientation, the converse is true. In Figure 1 it can be appreciated that the central portion of the inhibitor electron density comes from both inhibitor orientations, but the terminal portions of the density are from one or the other inhibitor molecule and not the sum of the two molecules. Although they appear superficially the same (Figure 1), upon closer examination, the C and D inhibitor conformations are clearly not identical. Figure 4 shows the conformations of C and D after superposition of A and B protein monomers. The largest change is seen in the orientation of the cyclohexyl rings; however, of equal importance may be the different relative locations of the N-terminal acetyl group (OT1) and the carbonyl oxygen atoms (O3 and O4). Atomic nomenclature for the inhibitor molecule is specified in Figure 5.

Interaction between the Inhibitor and the Protein Molecule. Perhaps predictably, the hydrogen bonding between the inhibitor and the protein is different for the various enzymes. We also observed hydrogen bond differences for the C and D orientations of the inhibitor. On the basis of consensus hydrogen bonds between the backbone of peptide inhibitors and the HIV-1 protease dimer (Wlodawer & Erickson, 1993), inhibitor U-89360E would be expected to interact with Gly 27 O on the N-terminal side of the active site and with Gly 27 O, Asp 29 N, Gly 48 O, and Gly 48 N on the C-terminal side. Figure 5, a diagram of observed hydrogen bond interactions, shows the presence of these bonds with two exceptions. Neither of the mutant structures has the N-terminal interaction with Gly 27 O for the C inhibitor orientation. The wild-type structure does not make the H-bond to Gly 48 O in the C orientation. Of course,

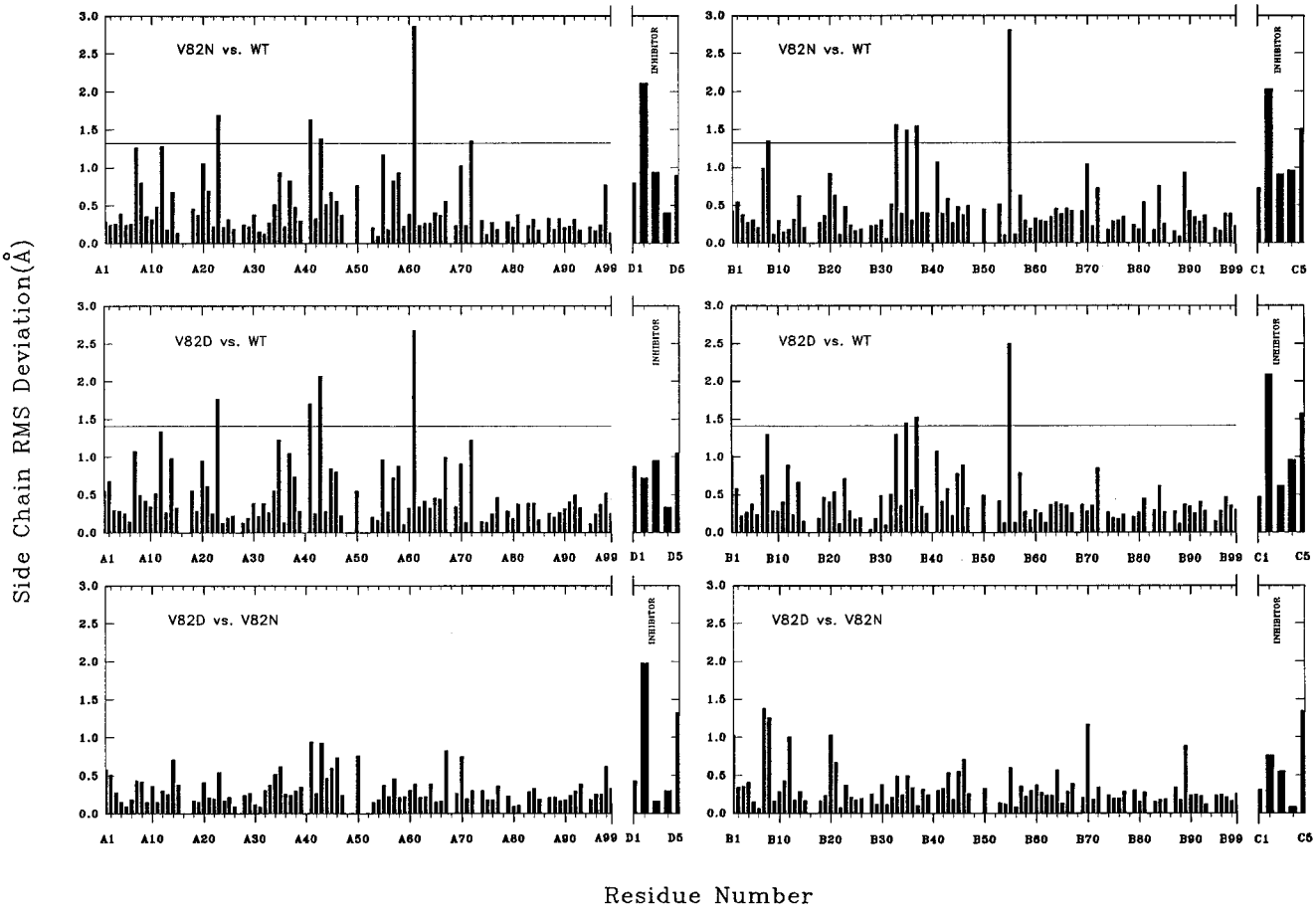

FIGURE 3: Side chain deviations among the three structures. Glycine residues and the mutated 82 side chain are omitted from this analysis. The horizontal lines represent the level of significant deviation (2σ above the mean deviation).

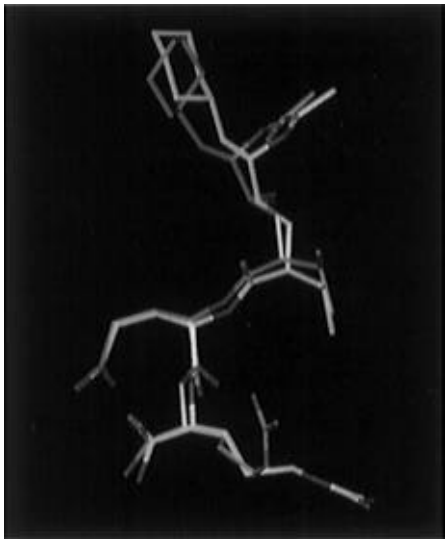

FIGURE 4: Superposition of the inhibitor conformations C (yellow) and D (green). The inhibitor conformations are compared after A and B protein monomers were aligned by rigid body superposition. The conformations from the V82D crystal structure are shown.

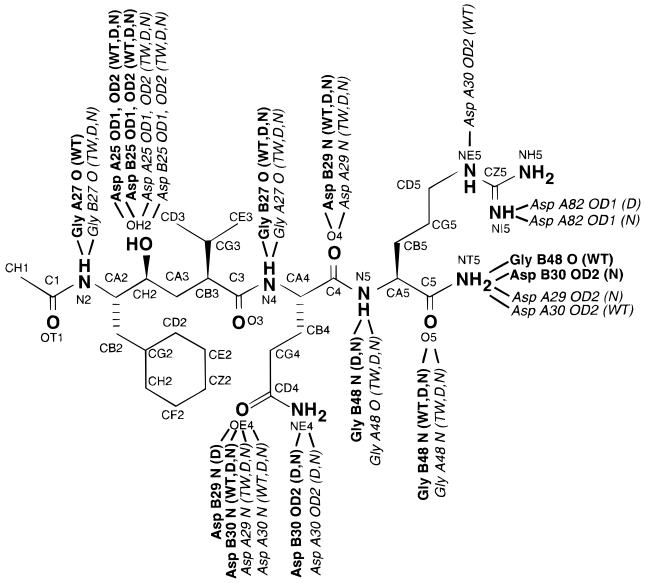

FIGURE 5: Diagrammatic presentation of hydrogen-bonding patterns between inhibitor and protein molecules. The hydrogen bonds shown are specified by chemically feasible bond angles and a distance between the two electronegative atoms between 2.4 and 3.5 Å. Interactions to the C inhibitor are in bold and to the D inhibitor are italicized. Nomenclature for the inhibitor atoms is defined. The existence of the hydrogen bond in a particular crystal structure is indicated by the parenthetical WT for wild type, N for V82N, or D for V82D.

bonds to inhibitor side chains are a consequence of the unique inhibitor structure. In the present case, there is variability at all possible locations, viz., the Gln, Arg, and pseudo-C-terminus of the inhibitor.

Another means to evaluate enzyme−inhibitor binding is examination of the juxtaposition of the molecules and the consequent van der Waals interactions. Residue 82 in HIV-1 protease forms part of the wall of the P_1 binding pocket and shields the inhibitor cyclohexyl side chain from solvent. The 82 side chain does not have any intermolecular contacts in the crystal. We observed significant differences in the $F_o - F_o$ difference maps between the wild-type enzyme and the mutants (Figure 6). These analyses provide unbiased

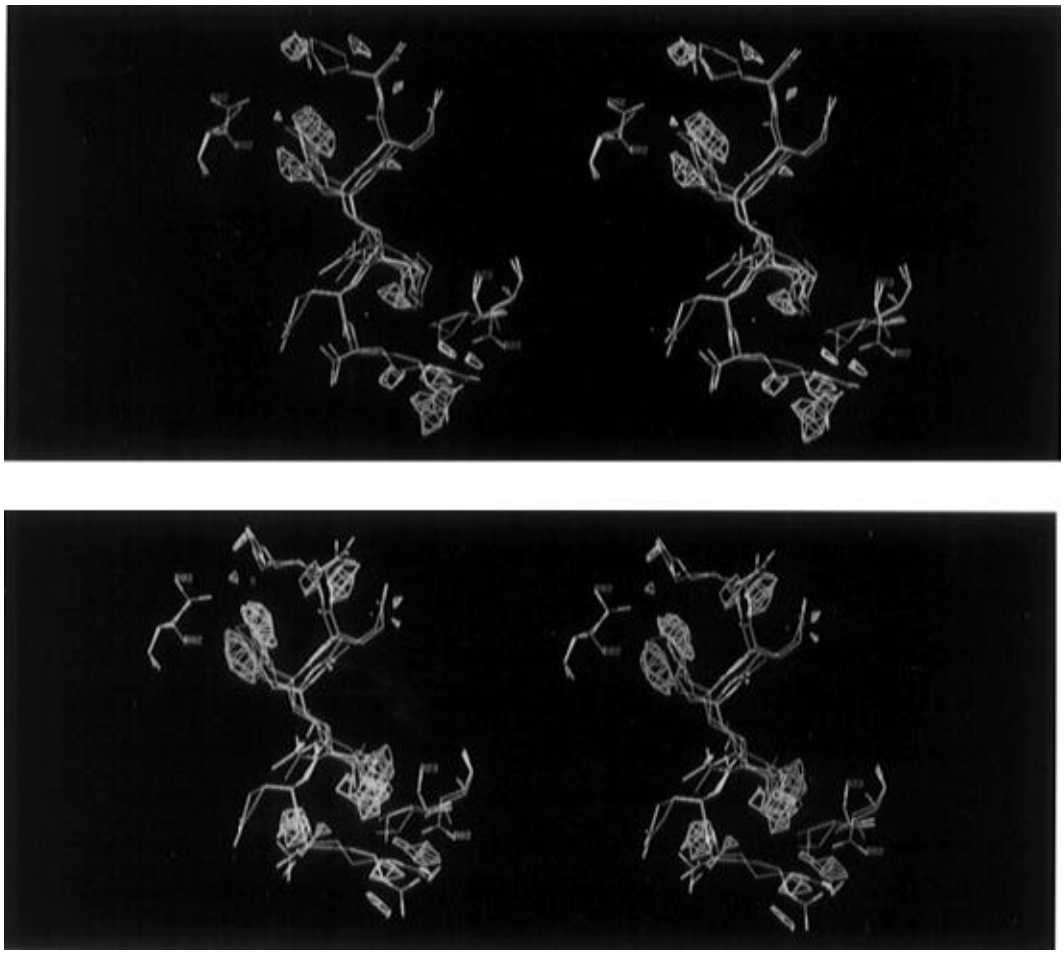

FIGURE 6: Difference maps to demonstrate inhibitor positional change upon mutation. Electron density contours are from $|F_o$(wild type)$|$ $-$ $|F_o$(mutant)$|$ difference maps. Map contours are only shown within 1.0 Å of the inhibitor molecules. The map contour level is $\pm 2.5\sigma$. (A, top) The wild-type and V82D mutant models are in red and green, respectively. Positive contours are in pink and negative are in yellow. (B, bottom) The wild-type and V82N mutant models are in red and blue, respectively. Positive contours are in pink and negative are in light blue.

evidence that the inhibitor binding to the mutants is different from that of the wild-type enzyme. The mutation of Val 82 to either Asp or Asn results in increased side chain size. To accommodate this change in the mutant enzymes, there is a repositioning of the inhibitor cyclohexyl group in the P_1 and P_1' binding pockets as well a change of the protein backbone at residue 82. Even though this conformational adaptation occurs, interactions in the mutant crystal structures are not nearly as favorable as those of the wild-type enzyme (Figure 7). The overlap of mutant protein and inhibitor van der Waals volumes and juxtaposition of a charged (aspartic acid) or polar (asparagine) protein side chain with the inhibitor cyclohexyl side chain are energetically costly. These observations are consistent with the observed K_i's of 20, 560, and 2100 nM for U-89360E binding to wild-type, V82D, and V82N HIV-1 proteases, respectively (Lin *et al.*, 1995).

Finally, of possible importance to the analysis of this set of structures are two water-mediated enzyme−inhibitor stabilizing interactions. In the consensus hydrogen bonding for HIV-1 protease to inhibitors, there is a water molecule which bridges the inhibitor carbonyl oxygen atoms which flank the "scissile" bond. This water molecule also accepts hydrogen atoms from the backbone amide groups of residue Ile 50 near the tips of the active site flaps of HIV-1 protease. The result is an attachment between the active side flap and the bound inhibitor which, presumably, also occurs for the substrates. This water molecule is clearly identifiable in the wild-type and V82N structures but is either not present or

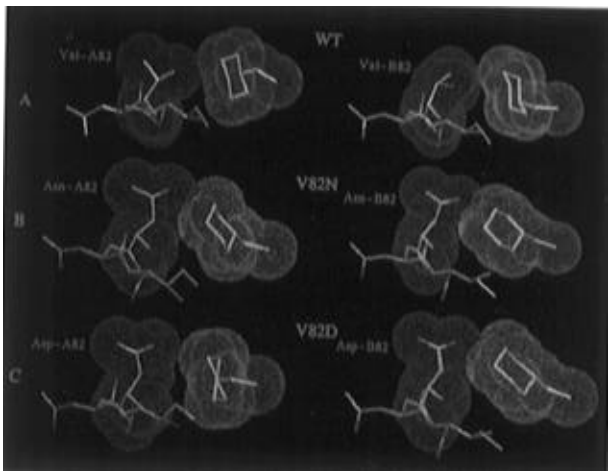

FIGURE 7: Van der Waals surface contacts for the interaction of the inhibitor molecules and protein side chains. Pink and blue contours represent inhibitor and protein surfaces, respectively. Default values from the graphics program O were used to define the surfaces. The view in each picture minimizes the observable overlap. The overlap of van der Waals volumes has been calculated according to Lee and Richards (1971) and is indicated for each complex. (A) Wild type, no overlap, (B) V82D, 1.12 Å^3 overlap, and (C) V82N, 3.43 Å^3 overlap.

of very low occupancy in the V82D structure. Baca and Kent (1993) reported that if the relevant amide −CONH− linkage of HIV-1 protease is changed to an isosteric thioester −COS−, the predominant kinetic effect is on k_{cat}. However,

in that case a decrease in k_{cat} was observed. Also, in each of the mutant structures, there is a water molecule bridging B51 N and A79 O. This is another interaction which tends to hold the flap in a closed position attached to the inhibitor. The absence of this water molecule in the wild-type structure is a consequence of the variable orientation of the 50−51 peptide bond in the B monomer (see above Description of the Protein Structures).

Analysis and Conclusions. Study of these three complexes may provide useful data to aid in understanding the phenomenon of escape mutation on an atomic level. As has been pointed out, escape from an inhibitor usually will be the result of a combination of decreased potency of inhibitor binding coupled with sustained or enhanced catalytic capability of the mutant enzyme. The analyses summarized in Figures 5−7 are consistent with the relative inhibitor binding constants for these mutant enzymes. The importance of mutation in the HIV-1 protease flap to alteration of the catalytic capability (k_{cat}/K_m) has been acknowledged by others (Chen *et al.*, 1995). We observed mutation-induced changes in the polypeptide backbone in two regions (residues 35−41 and residues 67 and 68) which might logically be related to flap mobility. Also, a water molecule usually provides stabilization for the enzyme−inhibitor complex by bridging the flap to the inhibitor. The absence of this molecule in the V82D complex could foster increased catalytic capability. Of course, the energetics of either binding or catalysis are a composite of a multitude of interactions so that the kinetic variation observed among the HIV-1 protease mutants results from the summation of many interactions and may not be attributable to any particular structural characteristic.

ACKNOWLEDGMENT

The authors thank Marcus Dehdarani for assisting in preparation of the enzymes, Dr. W. L. Thaisrivongs and Dr. R. L. Heinrikson for the gift of inhibitor U-89360E, and Dr. Vladimir Nauchitel for several enlightening discussions.

REFERENCES

Adbel-Meguid, S. S., Zhao, B., Murthy, K. H. M., Winborne, E., Choi, J.-K., DesJarlasi, R. L., Minnich, M. D., Culp, J. S., Debouck, C., Tomaszek, T. A., Jr., Meek, T. D., & Dreyer, G. B. (1993) *Biochemistry 32,* 7972−7980.

Ashorn, P., McQuade, T. J., Thaisrivongs, S., Tomasselli, A. G., Tarpley, W. G., & Moss, B. (1990) *Proc. Natl. Acad. Sci. U.S.A. 87,* 7472−7476.

Baca, M., & Kent, S. B. H. (1993) *Proc. Natl. Acad. Sci. U.S.A. 90,* 11638−11642.

Bailey, S. (1994) *Acta Crystallogr. D50,* 760−763.

Baldwin, E. T., Bhat, T. N., Liu, B., Pattabiraman, N., & Erickson, J. W. (1995) *Nat. Struct. Biol. 2,* 244−249.

Bernstein, F. C., Koetzle, T. F., Williams, G. J. B., Meyer, E. F., Brice, M. D., Rodgers, J. R., Kennard, O., Shimanouchi, T., & Tatumi, M. (1977) *J. Mol. Biol. 112,* 535−542.

Chen, Z., Li, Y., Schock, H. B., Hall, D., Chen, E., & Kuo, L. C. (1995) *J. Biol. Chem. 270,* 21433−21436.

Condra, J. H., Schleif, W. A., Blahy, O. M., Gabryelski, L. J., Graham, D. J., Quintero, J. C., Rhodes, A., Robbins, H. L., Roth, E., Shivaprakash, M., Titus, D., Yang, T., Teppler, H., Squires, K. E., Deutsch, P. J., & Emini, E. A. (1995) *Nature 374,* 569−571.

Debouck, C., & Metcalf, B. W. (1990) *Drug Dev. Res. 21,* 1−17.

Erickson, J. W. (1995) *Nat. Struct. Biol. 2,* 523−529.

Erickson, J. W., Neidhart, D. J., VanDrie, J., Kempf, D. J., Wang, X. C., Norbeck, D., Plattner, J. J., Rittenhouse, J. W., Turon, M., Wileburg, N., Kohlbrenner, W. E., Simmer, R., Helfrich, R., Paul, D. A., & Knigge, M. (1990) *Science 249,* 527−533.

Fitzgerald, P. M. D., McKeever, B. M., VanMiddlesworth, J. F., Springer, J. P., Heimbach, J. C., Leu, C.-T., Herber, W. K., Dixon, R. A. F., & Drake, P. L. (1990) *J. Biol. Chem. 265,* 14209−14219.

Gulnik, S. V., Suvorov, L. I., Liu, B., Yu, B., Anderson, B., Mitsuya, H., & Erickson, J. (1995) *Biochemistry 34,* 9282−9287.

Harte, W. E., Jr., Swaminathan, S., Mansuri, M. M., Martin, J. C., Rosenberg, I. E., & Beveridge, D. L. (1990) *Proc. Natl. Acad. Sci. U.S.A. 87,* 8864−8868.

Ho, D. D., Neumann, A. U., Perelson, A. S., Chen, W., Leonard, J. M., & Markowitz, M. (1995) *Nature 373,* 123−126.

Huff, J. R. (1991) *J. Med. Chem. 34,* 2305−2314.

Ido, E., Han, H., Kezdy, F. J., & Tang, J. (1991) *J. Biol. Chem. 266,* 24359−24366.

Jones, T. A. (1978) *J. Appl. Crystallogr. 11,* 268−272.

Jones, T. A., Zou, J.-Y., Cowna, S. W., & Kjeldgaard, M. (1991) *Acta Crystallogr. A47,* 110−119.

Kempf, D. J., Norbeck, D. W., Codacovi, L., Wang, X. C., Kohlbrenner, W. E., Wideburg, N. E., Paul, D. A., Knigge, M. F., Vasavanonda, S., Craig-Kennard, A., Saldivar, A., Rosenbrook, W., Jr., Clement, J. J., Plattner, J. J., & Erickson, J. (1990) *J. Med. Chem. 33,* 2687−2689.

Kohl, N. E., Emini, E. A., Schleif, W. A., Davis, L. J., Heimbach, J. C., Dixon, R. A. F., Scolnick, E. M., & Sigal, I. S. (1988) *Proc. Natl. Acad. Sci. U.S.A. 85,* 4686−4690.

Lam, P. Y. S., Jadhav, P. K., Eyermann, C. J., Hodge, C. N., Ru, Y., Bacheler, L. T., Meek, J. L., Otto, M. J., Rayner, M. M., Wong, Y. N., Chang, C.-H., Weber, P. C., Jackson, D. A., Sharpe, T. R., & Erickson-Viitanen, S. (1994) *Science 263,* 380−384.

Laskowski, R. A., MacArthur, M. W., Moss, D. S., & Thornton, J. M. (1993) *J. Appl. Crystallogr. 26,* 283−291.

Lee, B., & Richards, F. M. (1971) *J. Mol. Biol. 55,* 370−400.

Lin, Y., Lin, X., Hong, L., Foundling, S., Heinrikson, R. L., Thaisrivongs, S., Leelamanit, W., Raterman, D., Shah, M., Dunn, B. M., & Tang, J. (1995) *Biochemistry 34,* 1143−1152.

Loeb, D. D., Swanstrom, R., Everitt, L., Manchester, M., Stamper, S. E., & Hutchinson, C. A., III (1989) *Nature 340,* 397−400.

Mellors, J. W., Larder, B. A., & Schinazi, R. F. (1995) *Intern. Antiviral News 3,* 8−13.

Murthy, K. H. M., Winborne, E. L., Minnich, M. D., Culp, J. S., & Debouck, C. (1992) *J. Biol. Chem. 267,* 22770−22778.

Nicholson, L. K., Yamazaki, T., Torchia, D. A., Grzesiek, S., Bax, A., Stahl, S. J., Kaufman, J. D., Wingfield, P. T., Lam, P. Y. S., Jadhav, P. K., Hodge, C. N., Domaille, P. J., & Chang, C.-H. (1995) *Nat. Struct. Biol. 2,* 274−280.

Peng, C., Ho, B. K., Chang, T. W., & Chang, N. T. (1989) *J. Virol. 63,* 2550−2555.

Petteway, S. R., Jr., Dreyer, G. B., Meek, T. D., Metcalf, B. W., & Lambert, D. M. (1991) in *AIDS Research Review* (Koff, W. C., Wong-Staal, F., & Kennedy, R. D., Eds.) pp 267−288, Marcel Dekker, New York.

Ridky, T., & Leis, J. (1995) *J. Biol. Chem. 270,* 29621−29623.

Roberts, N. A., Martin, J. A., Kinchington, D., Broadhurst, A. V., Craig, J. C., Duncan, I. B., Galpin, S. A., Handa, B. K., Kay, J., Krohn, A., Lambert, R. W., Merrett, J. H., Mills, J. S., Parkes, K. E. B., Redshaw, S., Ritchie, A. J., Taylor, D. L., Thomas, G. J., & Machin, P. J. (1990) *Science 248,* 358−361.

Tang, J., & Hartsuck, J. A. (1995) *FEBS Lett. 367,* 112−116.

Tomasselli, A. G., Howe, W. J., Sawyer, T. K., Wlodawer, A., & Heinrikson, R. L. (1991) *Chim. Oggi (Chemistry Today) 9,* 6−27.

Vacca, J. P., Guare, J. P., deSolms, S. J., Sanders, W. M., Giuliani, E. A., Young, S. D., Darke, P. L., Zugay, J., Sigal, I. S., Schleif, W. A., Quintero, J. C., Emini, E. A., Anderson, P. S., & Huff, J. R. (1991) *J. Med. Chem. 34,* 1225−1228.

Wei, X., Ghosh, S. K., Taylor, M. E., Johnson, V. A., Emini, E. A., Deutsch, P., Lifson, J. D., Bonhoeffer, S., Nowak, M. A., Hahn, B. H., Saag, M. S., & Shaw, G. M. (1995) *Nature 373,* 117−122.

Wlodawer, A., & Erickson, J. W. (1993) *Annu. Rev. Biochem. 62,* 543−585.

BI960481S